Chapter 3

TIO_2-PHOTOCATALYZED AS(III) OXIDATION IN AQUEOUS SUSPENSIONS: REACTION KINETICS AND EFFECTS OF ADSORPTION

* Adapted from Ferguson et al., 2005. *Environmental Science & Technology*, vol. 39, no. 6, pp. 1880-1886.

3.1 Abstract

Oxidation of arsenite, As(III), to arsenate, As(V), is required for the efficient removal of arsenic by many water treatment technologies. The photocatalyzed oxidation of As(III) on titanium dioxide, TiO_2, offers an environmentally benign method for this operation. In this study, we explore the efficacy and mechanism of TiO_2-photocatalyzed As(III) oxidation at circumneutral pH and over a range of As(III) concentrations approaching those typically encountered in water treatment systems.

Adsorption (in the dark) of both As(III) and As(V) on Degussa P-25 TiO_2 was examined at pH 6.3 over a range in dissolved arsenic concentrations, $[As]_{diss}$, of 0.10 to 89 μM and 0.2 or 0.05 g L^{-1} TiO_2 (for As(III) and As(V), respectively). Adsorption isotherms generally followed the Langmuir-Hinshelwood model with As(III) exhibiting an adsorption maxima of 32 μmol g^{-1}. As(V) adsorption did not reach a plateau under the experimental conditions examined; the maximum adsorbed concentration observed was 130 μmol g^{-1}. The extent of As(III) and As(V) adsorption observed at the beginning and end of the kinetic studies was consistent with that observed in the adsorption isotherms.

Kinetic studies were performed in batch systems at pH 6.3 with 0.8-42 μM As(III) and 0.05 g L^{-1} TiO_2; complete oxidation of As(III) was observed within 10-60 min using

365 nm radiation. The observed effect of As(III) concentration on reaction kinetics was consistent with surface saturation at higher concentrations. Addition of phosphate at 0.5-10 μM had little effect on either As(III) sorption or its photooxidation rate but did inhibit adsorption of the product As(V). The selective use of hydroxyl radical quenchers and superoxide dismutase demonstrated that superoxide, $O_2^{\bullet -}$, plays a primary role in the oxidation of As(III) to As(V).

3.2 Introduction

Since arsenic (As) is a constituent of the earth's crust, elevated concentrations of As in groundwater can occur as a result of weathering processes. Exposure to As in drinking water is associated with increased risk of bladder, liver, kidney, and skin cancers (Korte and Fernando 1991; Smith et al. 2002). To reduce these risks, the U.S. drinking water standard for As was revised in 2001. It is estimated that thousands of water supply systems will need to implement technologies for arsenic treatment in order to comply with the revised standard of 10 μg L^{-1} (0.13 μM) by January 2006 (Dambies et al. 2002).

Arsenic in groundwater occurs primarily in inorganic form, either as arsenite, As(III), or arsenate, As(V). As(V) can be efficiently removed by common water treatment methods, such as coagulation with ferric chloride or alum, or use of activated alumina, anion exchange resins, or iron-based filter media. However, removal of As(III) by such processes can be quite variable and is often substantially less efficient (McNeill and Edwards 1995b; Hering et al. 1996; Hering et al. 1997; McNeill and Edwards 1997). Pre-oxidation of As(III) to As(V) thus enhances arsenic removal by many treatment

processes (Sorg and Logsdon 1978). Oxidation of As(III) to As(V) can be accomplished by several oxidants that are conventionally used in water treatment, including chlorine, permanganate, and ozone (Ghurye and Clifford 2001). Titanium dioxide (TiO_2) photocatalysis, although not conventionally used in drinking water treatment, offers an environmentally benign method of As(III) oxidation.

TiO_2 photocatalysis is commonly used for the photodegradation of aqueous and gas phase pollutants due to its low cost, stability with respect to corrosion, and biological and chemical inertness. Upon the absorption of sufficiently energetic light ($\lambda < 387$ nm) by TiO_2, an electron is promoted to the higher energy conduction band (CB), leaving a positively charged hole in the valence band (VB) (Table 3.1, reaction 1). The electron and hole can migrate to the surface of the semiconductor, where they are trapped by surface titanol groups (reactions 2-3). Charge recombination, either in the bulk (reaction 4) or at the surface (reactions 5-6) decreases the efficiency of photocatalyzed reactions. Electrons and holes that do not recombine can react to reduce and oxidize chemical species at the TiO_2 surface. In aerated solutions, oxygen serves as the primary electron acceptor (reaction 7), generating superoxide radical. Superoxide may self-react via disproportionation (reaction 12) into H_2O_2 and O_2, or it may be further reduced at the surface (reaction 8), also yielding H_2O_2. While adsorbed H_2O_2 may react either with an electron or a hole (reactions 9-10), holes can also oxidize adsorbed hydroxide, forming hydroxyl radical (reaction 11). Note that to achieve reasonable photoefficiency in a TiO_2/UV system, both electrons and holes must have substrates with which to react at the particle surface (Hoffmann et al. 1995).

Table 3.1. Reactions involved in TiO_2-photocatalyzed As(III) oxidation.

Charge separation

$$TiO_2 + h\nu \rightarrow e_{CB}^- + h_{VB}^+ \quad (1)$$

Surface trapping

$$\equiv Ti^{IV}OH + h_{VB}^+ \rightarrow \{\equiv Ti^{IV}OH^\bullet\}^+ \quad (2)$$

$$\equiv Ti^{IV}OH + e_{CB}^- \leftrightarrow \equiv Ti^{III}OH \quad (3)$$

Recombination

$$e_{CB}^- + h_{VB}^+ \rightarrow \text{heat} \quad (4)$$

$$e_{CB}^- + \{\equiv TiOH^\bullet\}^+ \rightarrow \equiv TiOH \quad (5)$$

$$h_{VB}^+ + \equiv Ti^{III}OH \rightarrow \equiv Ti^{IV}OH \quad (6)$$

Interfacial charge transfer: Reactive O species

$$O_2 + e_{CB}^- \rightarrow O_2^{\bullet-} \quad (7)$$

$$O_2^{\bullet-} + 2H^+ + e_{CB}^- \rightarrow H_2O_2 \quad (8)$$

$$H_2O_2 + e_{CB}^- \rightarrow {}^\bullet OH + OH^- \quad (9)$$

$$H_2O_2 + h_{tr}^+ \rightarrow HO_2^\bullet + H^+ \quad (10)$$

$$H_2O_{ads} + h_{VB}^+ \rightarrow H^+ + {}^\bullet OH_{ads} \quad (11)$$

$O_2^{\bullet-}$ Disproportionation

$$2O_2^{\bullet-} + 2H^+ \rightarrow H_2O_2 + O_2 \quad (12)$$

Interfacial charge transfer: As species

$$As(OH)_3 + \{\equiv TiOH^\bullet\}^+ \rightarrow As^{IV}(OH)_3^{\bullet+} \quad (13)$$

$$As(OH)_3 + {}^\bullet OH_{ads} + H^+ \rightarrow As^{IV}(OH)_3^{\bullet+} + H_2O \quad (14)$$

$$As(OH)_3 + O_2^{\bullet-} + 2H^+ \rightarrow As^{IV}(OH)_3^{\bullet+} + H_2O_2 \quad (15)$$

$$As^{IV}(OH)_3^{\bullet+} + \{\equiv TiOH^\bullet\}^+ + H_2O \rightarrow \equiv TiOH + H_2AsO_4^- + 3H^+ \quad (16)$$

$$As^{IV}(OH)_3^{\bullet+} + {}^\bullet OH_{ads} \rightarrow H_2AsO_4^- + 2H^+ \quad (17)$$

$$As^{IV}(OH)_3^{\bullet+} + O_2 + H_2O \rightarrow H_2AsO_4^- + O_2^{\bullet-} + 3H^+ \quad (18)$$

TiO_2 photocatalysis has been shown to be effective in oxidizing As(III) to As(V) in the presence of oxygen (Yang et al. 1999; Bissen et al. 2001; Lee and Choi 2002; Jayaweera et al. 2003; Ryu and Choi 2004). Despite differences in applied light

intensities and other experimental conditions, the photocatalyzed oxidation of As(III) to As(V) in batch systems has generally been observed to go to completion on timescales of <10-100 min. Most of these previous studies were conducted with very elevated initial As(III) concentrations (≥500 μM) and TiO_2 concentrations between 0.25 and 2 g L^{-1} (Yang et al. 1999; Lee and Choi 2002; Ryu and Choi 2004). In one study, the initial As(III) concentration was varied from 0.1 to 130 μM with 0.001-0.05 g L^{-1} TiO_2; these authors observed a pseudo first-order dependence of the reaction on the dissolved As(III) concentration and a linear dependence of the pseudo first-order rate coefficient on the TiO_2 concentration (Bissen et al. 2001). Although the pH conditions for this study were not stated, the authors reported that no pH dependence was observed between pH 5 and 9. Other studies were conducted at pH 3 (Lee and Choi 2002; Ryu and Choi 2004), 7 (Jayaweera et al. 2003), and 9 (Yang et al. 1999; Lee and Choi 2002; Ryu and Choi 2004). The photooxidation rate at pH 3 has been observed to be accelerated by addition of humic acid, Fe(III) (Lee and Choi 2002), polyoxometalates, and fluoride (Ryu and Choi 2004). Platinization of the TiO_2 enhanced As(III) photooxidation at both pH 3 and 9. Ryu and Choi (2004) observed deceleration of the photocatalysis rate with the substitution of carbon tetrachloride for oxygen as the electron acceptor and by addition of superoxide dismutase, and Lee and Choi (2002) found that the photocatalysis rate was unaffected by the addition of *t*-butanol, a hydroxyl radical scavenger. Thus, Choi and co-workers concluded that the TiO_2 photocatalyzed oxidation of As(III) proceeds predominantly by reaction of As(III) with a superoxide radical generated at the TiO_2 surface (reaction 15) rather than by reaction with a trapped hole (reaction 13) (Szczepankiewicz et al. 2000; Szczepankiewicz et al. 2002a; Szczepankiewicz et al.

2002b) or surface hydroxyl radical (reaction 14). Note that the resulting As(IV) radical is expected to be quickly oxidized to As(V), either by reaction with a trapped hole or hydroxyl radical (reactions 16-17) or by molecular oxygen (reaction 18). Reduction of As(IV) or As(V) by a trapped electron (Szczepankiewicz et al. 2000; Szczepankiewicz et al. 2002a; Szczepankiewicz et al. 2002b) is also possible, but such back-reactions are not likely to play a major role due to competition with molecular oxygen. In the absence of oxygen, reduction of As(V) to As(0) has been reported to occur at pH 3 (Yang et al. 1999).

Since TiO_2-photocatalyzed reactions occur at the TiO_2 surface, adsorption of the reacting species (e.g., As(III) and O_2) is a critical aspect of the overall reaction. Although the structure of As(III) and As(V) surface species has not been examined for TiO_2 specifically, such studies have been conducted with iron and aluminum oxides using both spectroscopic techniques, such as X-ray absorption and vibrational spectroscopy, and macroscopic observations of As sorption as reviewed by Hering and Dixit (2004). Both As(III) and As(V) form inner-sphere surface complexes on iron oxides; spectroscopic studies show these complexes to be largely binuclear and bidentate though, depending on surface coverage, monodentate complexes may also be formed (Waychunas et al. 1993; Waychunas et al. 1995; Fendorf et al. 1997). Similar inner-sphere surface complexes have been proposed for As(V) on manganese (Foster et al. 2003) and aluminum (Arai et al. 2001; Goldberg and Johnston 2001) oxides, as well as for phosphate, an electronic analog of As(V), on TiO_2 (Connor and McQuillan 1999). In contrast, outer-sphere complexation has been proposed for As(III) on amorphous aluminum oxides (Goldberg

and Johnston 2001), although for γ-Al_2O_3 inner-sphere bidentate binuclear complexes may be formed at pH ≤ 5.5 (Arai et al. 2001).

In this work, we examine more closely the role of As adsorption during the photocatalytic oxidation of As(III). In particular, we explore the effect of surface reactions on the observed dependence of reaction rates on the dissolved As(III) concentration and on the efficiency of various reaction inhibitors. Our goal is to explore a range of conditions that more closely approximate typical conditions encountered during drinking water treatment.

3.3 Materials and Methods

3.3.1 Chemicals

Chemicals used for preparation of arsenic stock solutions were As_2O_3 (Aldrich) or $NaAsO_2$ (Baker Analyzed) for As(III) and $Na_2HAsO_4 \cdot 7H_2O$ (Sigma) for As(V). $NaNO_3$ (Mallinckrodt AR), *tert*-butyl alcohol (Baker Analyzed), CCl_4 (Aldrich), and $Na_2HPO_4 \cdot H_2O$ (EM) were used as received. Degussa P25 titanium dioxide, with an average BET surface area of 50 $m^2\ g^{-1}$ and a PZC of 6.25 (Bourikas et al. 2001), was used for all experiments. 1.0 g L^{-1} stock suspensions of P25 TiO_2 were prepared and then sonicated for 20 minutes before use. A CCl_4 stock solution was prepared by adding excess CCl_4 to pre-boiled, N_2-sparged water; the CCl_4-saturated solution (5.1 mM based on solubility constant) was subsequently diluted to achieve a nominal concentration of 1 mM. Superoxide dismutase (Sigma, from bovine erythrocytes) solutions were prepared by dissolving 4-6 mg of the lyophilized powder in water and adding it to 200 mL of a

TiO_2 suspension, which produced ~100,000 units L^{-1}. All water used was distilled and deionized (Milli-Q, 18.2 MΩ•cm).

3.3.2 Photocatalysis

Suspensions containing 0.05 g L^{-1} TiO_2 were prepared with 0.005 M $NaNO_3$, which was added as a background electrolyte. Nitrate is not photoactive in the wavelength region studied regardless of the presence or absence of TiO_2 (Villars 1927; Bems et al. 1999). The TiO_2/$NaNO_3$ suspension was transferred into a Pyrex cell with a 200 mL capacity, 3 cell necks, and a quartz window (5.2 cm diameter). The cell necks were fitted with rubber septa through which a combination semi-micro pH electrode (Mettler Toledo InLab 422), gas dispersion tube, and gauge 13 needle (used for sampling) were inserted. The suspensions were continuously stirred and bubbled with air or ultra high purity N_2. As(III) was added to achieve the desired total concentration (As_T), and the suspension was stirred in the dark for 30 minutes to allow the system to attain sorption equilibrium. Suspension pH was adjusted to 6.3 with NaOH and HNO_3 (0.01–0.1 M) and maintained throughout the experiment by adding 10 μL aliquots of acid or base as needed.

For experiments conducted under N_2, the TiO_2 suspension was boiled during N_2 sparging for 20 minutes to remove residual O_2. After the solution cooled, it was transferred to the cell through Tygon tubing using excess N_2 pressure. Stock solutions of As(III) and $NaNO_3$ were added directly to the cell and were therefore not heated, but the resulting mixture was sparged with N_2 prior to TiO_2 suspension transfer and maintained under N_2 throughout the experiment.

The reaction mixtures were irradiated with an 8 W, 365 nm lamp (UVP Model UVL-28). The photon flux through the cell was 7.8×10^{16} photons s^{-1} as determined by ferrioxalate actinometry (Calvert and Pitts 1966). During photolysis, time-resolved aliquots were removed using a 10 mL syringe and immediately filtered through a 0.22 μm nitrocellulose membrane (Millipore) to remove TiO_2. All runs were performed at least twice, in most cases yielding results within 10% of each other.

3.3.3 Analytical Procedures

Arsenic speciation was determined by passing part of each sample through an anion exchange filter (3M Anion SR). At circumneutral pH, As(V) (pK_{a1} = 2.2, pK_{a2} = 7.0) is retained on the filter while As(III) (pK_{a1} = 9.1) passes through. Arsenic was quantified by ICP-MS (HP 4500) using a gallium internal standard in samples collected before and after anion exchange filtration to obtain concentrations of total dissolved arsenic ($[As]_{diss}$) and dissolved As(III) ($[As(III)]_{diss}$), respectively. Dissolved As(V) ($[As(V)]_{diss}$) was calculated by difference.

3.4 Results and Discussion

Experiments were conducted to better understand the relationship between As(III) sorption and photooxidation on TiO_2. Adsorption isotherms were generated for both As(III) and As(V) on P25 TiO_2, and were compared to measured $[As(III)]_{diss}$ and $[As(V)]_{diss}$ values to confirm the achievement of sorption equilibrium at the beginning and end of photooxidation experiments. The effects that a competitive sorbate, hydroxyl

radical quenchers, and superoxide-inhibiting conditions induced on the photooxidation rate were explored in further experiments.

3.4.1 Arsenic adsorption on TiO_2

Sorption isotherms for As(III) and As(V) on P25 TiO_2 show that, in the absence of light, As(V) is adsorbed to a greater extent than As(III) at pH 6.3 (Fig. 3.1). Over the concentration range in $[As]_{diss}$ examined, the adsorbed concentration of As(III) appears to reach a plateau but that of As(V) does not. The maximum adsorbed concentrations of As(III) and As(V) observed under these conditions were 32 and 130 μmol g^{-1} TiO_2, respectively.

An estimated density of surface hydroxyl groups ranging from 3.3 to 5.4 nm^{-2} (Erdem et al. 2001; Mueller et al. 2003) corresponds to between 7.8 and 13% of monolayer coverage for As(III) and between 33 and 55% for As(V). These values for surface coverage by As(III) and As(V) are sufficiently low that As could be adsorbed as binuclear surface complexes.

3.4.2 As(III) photooxidation kinetics

In the presence of TiO_2, air and UV light, As(III) is rapidly removed from solution at pH 6.3 while As(V) is produced. The dissolved As(V) concentration increases over time, leveling off at a concentration equal to or less than the initial dissolved As(III) concentration, $[As(III)]_{diss,\ 0}$. The difference between $[As(III)]_{diss,\ 0}$ and final dissolved As(V) concentration ($[As(V)]_{diss,\ final}$) is most pronounced for low As_T (Fig. 3.2a) and is negligible at high As_T (Fig. 3.2c). At the beginning of photooxidation experiments,

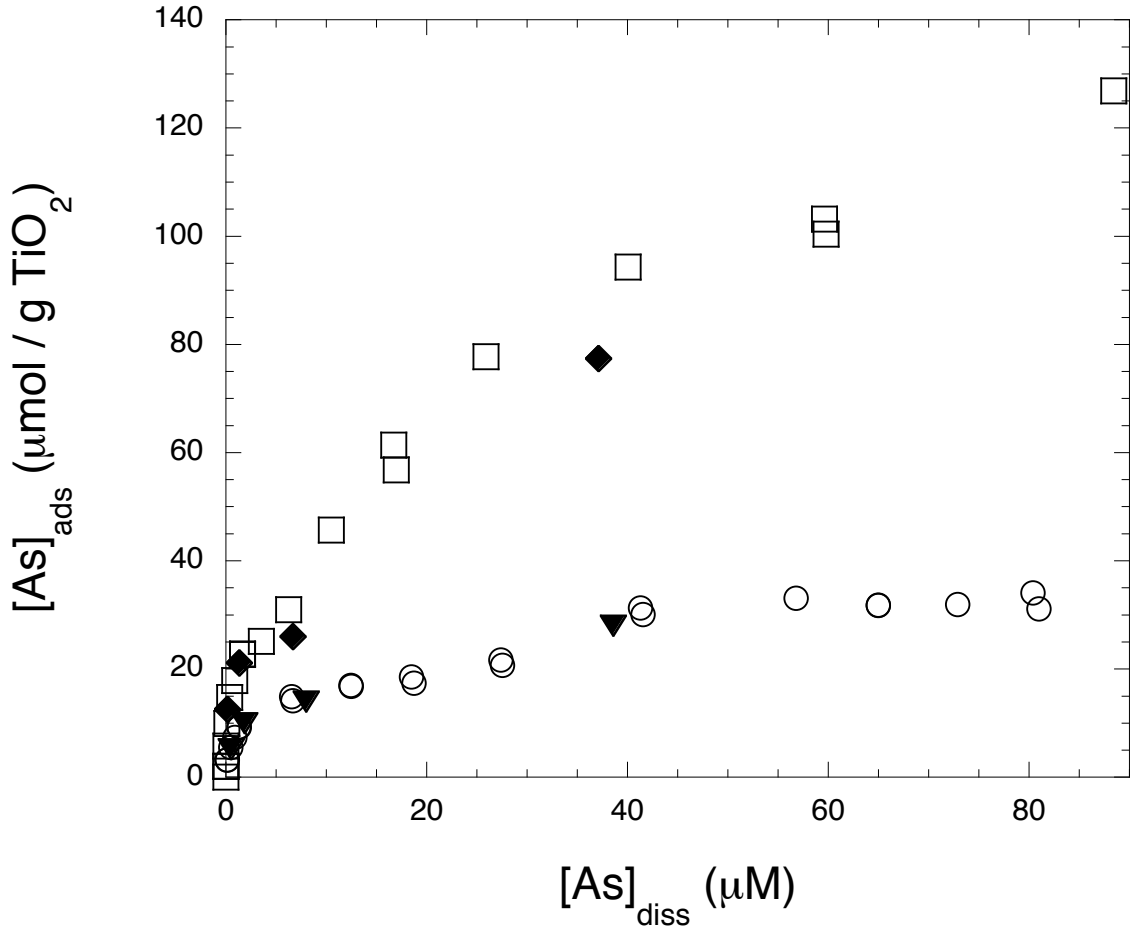

Figure 3.1. Adsorption isotherms for As(III) and As(V) on P25 TiO_2. Conditions: pH 6.3, 0.005 M $NaNO_3$, 0.20 g L^{-1} TiO_2 for As(III) (○) and 0.05 g L^{-1} TiO_2 for As(V) (□). Initial As(III) (▼) and final As(V) (◆) for photochemical experiments appear to be at sorption equilibrium.

where all As is present as As(III), the initial $[As(III)]_{diss}$ and adsorbed As(III) concentration, $[As(III)]_{ads}$, are consistent with the As(III) sorption isotherm (Fig. 3.1). Similarly, if we assume that all As has been oxidized to As(V) by the end of the reaction, the final $[As(V)]_{diss}$ and adsorbed As(V) concentration, $[As(V)]_{ads}$, are consistent with the As(V) sorption isotherm.

At 0.83 and 2.5 μM As_T, TiO_2-photocatalyzed As(III) oxidation exhibits pseudo first-order kinetics with respect to dissolved As(III) (Fig. 3.2b), consistent with previous observations by Bissen et al. (2001):

$$\frac{d[\text{As(III)}]_{\text{diss}}}{dt} = k_{obs}[\text{As(III)}]_{\text{diss}}$$

where k_{obs} is the observed rate coefficient. If $[As(III)]_{ads}$ and $[As(III)]_{diss}$ are assumed to be in pseudo-equilibrium, then

$$\frac{d[\text{As(III)}]_{\text{diss}}}{dt} = k_{ox}[\text{As(III)}]_{\text{ads}}$$

where k_{ox} is the rate coefficient for the photocatalyzed oxidation of adsorbed As(III). Because of surface saturation, however, $[As(III)]_{ads}$ and $[As(III)]_{diss}$ will be linearly related only in the linear portion of the isotherm. As surface saturation is approached, $[As(III)]_{ads}$ will remain constant even as $[As(III)]_{diss}$ increases. Thus the value of k_{obs} will not be constant, but will instead decrease with increasing $[As(III)]_{diss}$; deviation from pseudo first-order kinetics is expected under these conditions.

At As_T = 42 μM, the kinetic data are consistent with pseudo zero-order kinetics (Fig. 3.2c, d), which is expected for the plateau region of the isotherm. For As_T = 8.3 μM, the kinetic data are reasonably well fit as a pseudo first-order process (Fig. 2f) but the value of k_{obs} (2.6×10^{-3} s^{-1}) is less than that (4.8×10^{-3} s^{-1}) at As_T = 2.5 μM. In addition, the pseudo first-order fit is not dramatically better than a pseudo zero-order fit (Fig. 3.2e). These observations are consistent with a shift from pseudo first-order to pseudo zero-order kinetics.

TiO_2 photocatalyzed oxidation of As(III) also involves reduction of O_2 at the TiO_2 surface. Hence competition between O_2 and As(III) for sorption sites could result in a

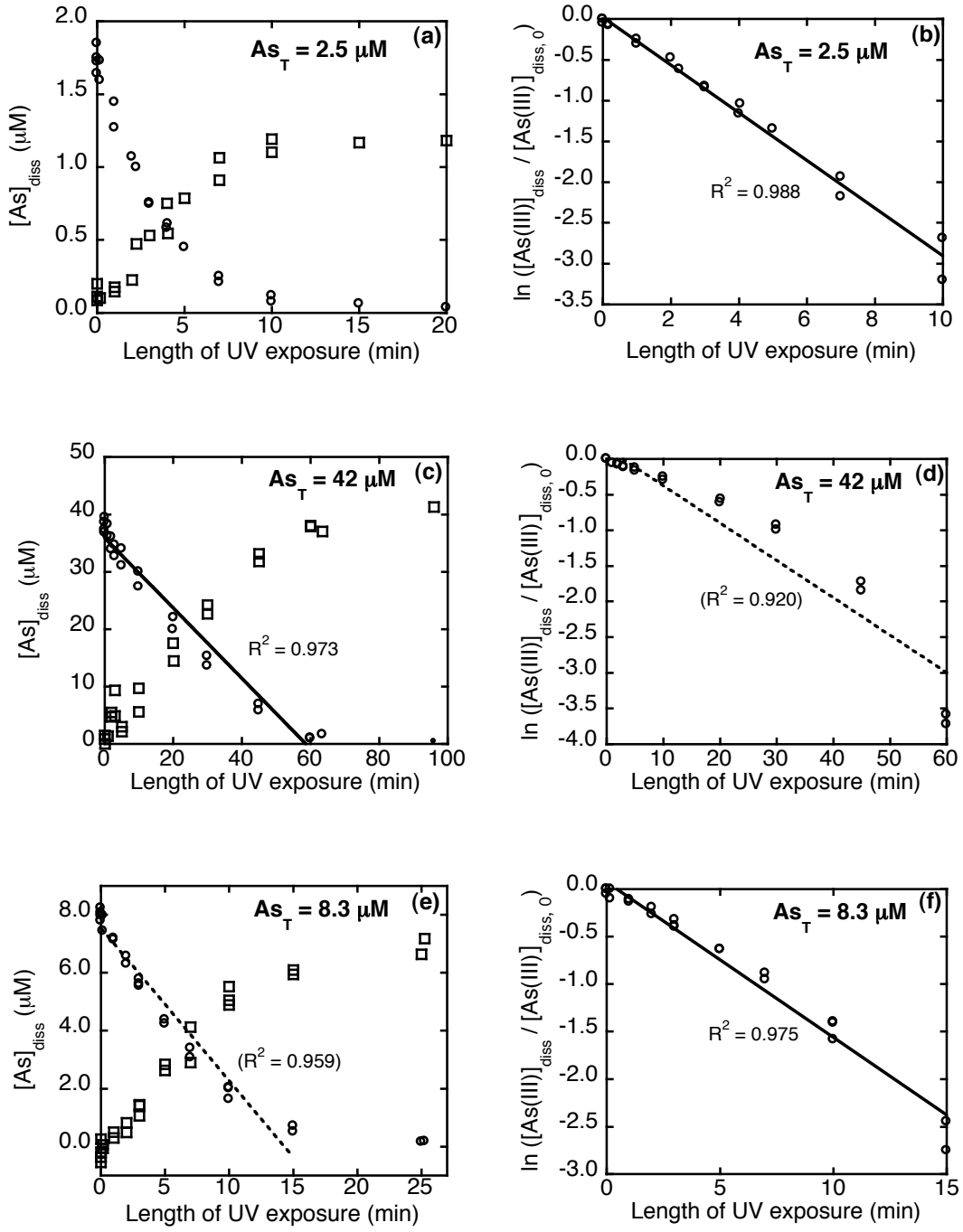

Figure 3.2. Loss of $[As(III)]_{diss}$ (○) and generation of $[As(V)]_{diss}$ (□) over exposure to UV irradiation for As_T = 2.5 (a), 42 (c), and 8.3 μM (e). Pseudo first order linearizations are shown for As_T = 2.5 (b), 42 (d), and 8.3 μM (f). Conditions: 0.05 g L^{-1} TiO_2, 0.005 M $NaNO_3$, pH 6.3.

decrease in the value of the k_{obs} with increasing $[As(III)]_{diss}$. Competitive sorption has been invoked to explain such observations for substrates including $CHCl_3$, 4-chlorophenol, and phenol (Hoffmann et al. 1995). In the case of As(III) photooxidation, however, effects of competition with O_2 are not apparent, possibly because the maximum adsorbed As(III) concentration is much lower than the surface hydroxyl group density for P25 TiO_2.

3.4.3 Effect of a competitive adsorbate

Phosphate, which is known to adsorb strongly to TiO_2 (Abdullah et al. 1990; Connor and McQuillan 1999), was added at varying concentrations in experiments with 0.83, 2.5, and 42 μM As_T to assess the effect of a competitive sorbate. At As_T = 42 μM, the values of k_{obs} are independent of phosphate concentration from 0–10 μM (k_{obs} = 0.74 ± 0.05 M s^{-1}, n = 4). At 0.83 and 2.5 μM As_T, the highest values of k_{obs} are obtained for ≤1 μM phosphate, but k_{obs} is fairly constant for phosphate concentrations between 3 and 10 μM (Table 3.2). This behavior is consistent with the relatively minor effect that phosphate in this concentration range has on As(III) sorption; initial As(III) sorption was decreased by ≤21%.

In contrast, dissolved As(V) concentrations are more strongly affected by phosphate addition. The final values of $[As(V)]_{diss}$ for experiments with 10 μM phosphate were significantly higher than those for corresponding experiments without phosphate (Table 3.2). As expected, in experiments with 42 μM As_T, the final values of $[As(V)]_{diss}$ were unaffected by the presence of phosphate since the surface was nearly saturated with arsenic at this concentration.

Table 3.2. Initial dissolved As(III), final dissolved As(V), and observed pseudo first-order As(III) photooxidation rate coefficients for different experimental conditions.

Experimental Conditions	**As_T (μM)**	**$[As(III)]_{diss, 0}$ (μM)**	**$[As(V)]_{diss, final}$ (μM)**	**k_{obs} (s^{-1})**	**% of $k_{obs\ (air, 1\ \mu M)}$**
Air-saturated	0.83	0.53	0.16	4.8×10^{-3}	100
	2.5	1.9	1.3	4.8×10^{-3}	100
	8.3	8.0	6.7	2.6×10^{-3}	54
Air / 0.5 μM PO_4	0.83	0.52	0.23	3.8×10^{-3}	79
	2.5	1.6	1.1	5.9×10^{-3}	124
Air / 1 μM PO_4	2.5	1.7	1.2	5.6×10^{-3}	117
Air / 3 μM PO_4	0.83	0.67	0.44	3.0×10^{-3}	63
Air / 5 μM PO_4	2.5	2.2	2.0	4.2×10^{-3}	87
Air / 10 μM PO_4	0.83	0.60	0.56	3.8×10^{-3}	78
	2.5	2.2	2.0	3.4×10^{-3}	71
Air / 0.001 M t-BuOH	2.5	1.9	1.3	4.8×10^{-3}	100
Air / 0.01 M t-BuOH	2.5	2.1	1.8	2.8×10^{-3}	58
Air / 0.1 M t-BuOH	0.83	0.83	0.37	2.1×10^{-3}	44
	2.5	2.2	1.8	2.1×10^{-3}	44
Air / 0.001 M 2-propanol	2.5	2.0	1.3	3.2×10^{-3}	67
Air / 0.1 M 2-propanol	2.5	2.5	1.9	2.5×10^{-3}	52
N_2-saturated	0.83	0.60	0.20	1.5×10^{-4}	3.1
N_2 / CCl_4	0.83	0.90	0.36	1.7×10^{-4}	3.6
Air / SOD	0.83	0.65	0.35	1.3×10^{-3}	27

3.4.4 Mechanism of As(III) photooxidation

As previously discussed, there are three potential mechanisms for As(III) oxidation in the presence of P25 TiO_2 and UV light: oxidation by hydroxyl radicals, by trapped holes, or by superoxide radicals. Tertiary butanol (*t*-BuOH) and 2-propanol, which are known $^{\bullet}OH$ radical scavengers, were used to test the first possibility. At both 0.83 μM and 2.5 μM As_T, the presence of 0.1 M *t*-BuOH decreased k_{obs} from 4.8×10^{-3} s^{-1} to 2.1×10^{-3} s^{-1} (Table 3.2). However, such a high concentration of a nonpolar solvent had the additional effect of inhibiting As(III) sorption. At As_T = 2.5 μM, the addition of 0.1 M *t*-BuOH decreased initial As(III) sorption by nearly half, and at 0.83 μM As_T there was hardly any As(III) adsorbed. When intermediate concentrations of *t*-BuOH were employed (0.01 and 0.001 M), the effect on As(III) sorption was diminished, and addition of 0.001 M *t*-BuOH had essentially no effect on either initial As(III) sorption or k_{obs}. Figure 3.3 shows the effect of [*t*-BuOH] on As(III) photooxidation for 2.5 μM As_T.

Even 0.001 M *t*-BuOH should be sufficient to act as a hydroxyl radical quencher in a system with only 0.05 g L^{-1} TiO_2 and micromolar levels of As(III). Therefore, it is likely that the effect of higher *t*-BuOH concentrations is due more to the decrease in As(III) sorption than to scavenging hydroxyl radicals. This interpretation corroborates the results of Lee and Choi (2002), who observed no effect of 0.53 M *t*-BuOH on the reaction of 500 μM As(III) with 1.5 g/L TiO_2. Under such conditions, the sorption capacity of the system is already exceeded, and thus only a small fraction of the total arsenite is adsorbed to the TiO_2. Consequently, the presence of *t*-BuOH would have only a minimal effect on As(III) sorption.

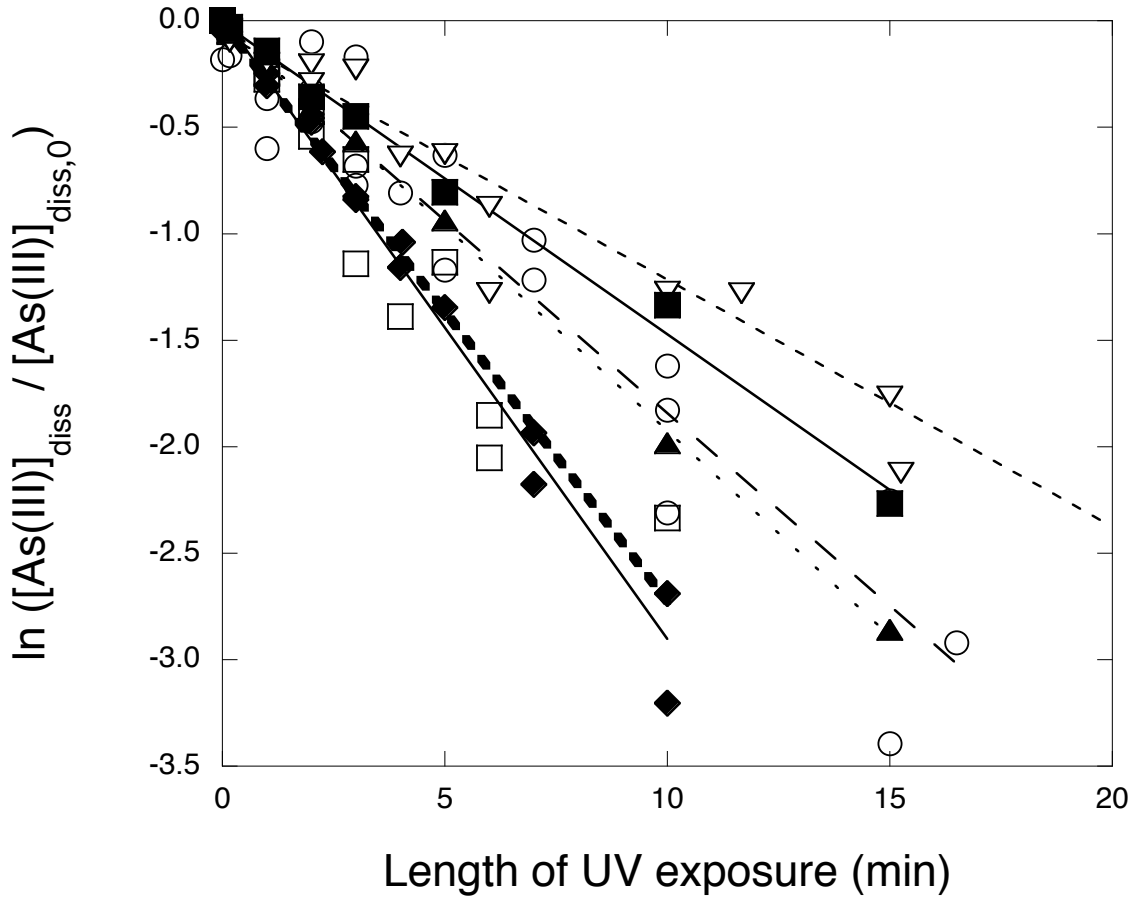

Figure 3.3. Effect of 0 M (◆), 0.001 M (□), 0.01 M (○), and 0.1 M (▽) *t*-BuOH as well as 0.001 M (▲) and 0.1 M (■) 2-propanol on photooxidation. Conditions: 2.5 μM As_T, pH 6.3, 0.05 g L^{-1} TiO_2, 0.005 M $NaNO_3$.

There is controversy in the literature as to whether *t*-BuOH adequately scavenges surface-bound hydroxyl radicals (Sun and Pignatello 1995; Minero et al. 2000b). Since the relative bulk of *t*-BuOH might prevent it from interacting with the TiO_2 surface, 2-propanol was used as an alternative $^{\bullet}OH$ scavenger. 2-propanol can serve as a quencher for both hydroxyl radicals and trapped holes (Choi and Hoffmann 1997; Minero et al. 2000b). The effect of 0.001 M 2-propanol on As(III) photooxidation was more

pronounced than that of 0.001 M *t*-BuOH, although this effect was still fairly small (Fig. 3.3).

Although 2-propanol is more likely than *t*-BuOH to scavenge surface-bound $^{\bullet}OH$, its use introduces a second confounding factor; 2-propanol is well known for causing current-doubling effects (Mandelbaum et al. 1999; Ohno et al. 2000). After donating an electron to the hydroxyl radical formed on illuminated TiO_2, the resulting α-hydroxyl radical may then inject a second electron into the TiO_2 conduction band. Thus, while the presence of 2-propanol may slow the reaction due to quenching of surface hydroxyl radicals, it may simultaneously enhance the reaction by providing excess conduction band electrons that can react to produce more superoxide. If TiO_2-photocatalyzed As(III) oxidation were due exclusively to reaction with superoxide, current-doubling by 2-propanol would be expected to enhance photooxidation. However, the extent of current doubling is dependent on many parameters, including the degree of doping, the nature of the solvent, dissolved oxygen availability, and the specific current doubling species (Hykaway et al. 1986; Mandelbaum et al. 1999), and the presence of Fe(III) ions has been shown to completely inhibit current doubling (Ohno et al. 2000). Given these many uncertainties, we are unable to argue against a superoxide-based oxidation mechanism in which molecular oxygen accepts a conduction band electron (Table 3.1, reaction 7), superoxide oxidizes As(III) to As(IV) (reaction 15), and As(IV) is subsequently oxidized to As(V) (reactions 16-18).

To address the role of superoxide anion, two methods were used to eliminate superoxide from the system. In the first method, the suspension was sparged with N_2, and CCl_4 was added as an alternate electron acceptor for O_2. The reaction was inhibited

almost entirely compared to air-purged samples (Fig. 3.4). The remaining slow reaction is likely due either to escape of lattice oxygen (Szczepankiewicz et al. 2000) or to trace O_2 diffusing into the system. The presence of CCl_4 did not enhance the N_2-sparged reaction, indicating that oxidation of As(III) by holes or surface-bound $^{\bullet}OH$ radicals does not occur to a significant degree.

The second method to eliminate superoxide was the addition of superoxide dismutase (SOD), which catalyzes reaction 12 but still allows O_2 to accept electrons or oxidize species directly. SOD is packaged with a phosphate buffer that contributed 2.7 μM phosphate under the conditions of the experiment, so an air-sparged system with excess phosphate (10 μM) is shown in Figure 3.4 for comparison. The presence of phosphate decreased initial As(III) sorption by 23% and slowed the reaction slightly, but the inhibitory effect of SOD was greater than can be explained solely by sorption competition between As(III) and phosphate (Fig. 3.4, Table 3.2). As(III) photooxidation in the presence of SOD confirms the observations of Ryu and Choi (2004) and supports their hypothesis that $^{\bullet}O_2^-$ plays a dominant role in As(III) photooxidation. Complete quenching of As(III) photooxidation by SOD was not observed either in this study or by Ryu and Choi (2004), who added SOD at concentrations up to 333 mg L^{-1} with 0.5 g L^{-1} TiO_2. They suggested that SOD might be unstable under UV illumination (Ryu and Choi 2004), but given the short irradiation periods and weak UV intensity compared to other work demonstrating gradual loss of SOD activity over time (Amalric et al. 1994), this is unlikely. Instead, the catalytic activity of SOD may be limited by its ability to bind successively to two $^{\bullet}O_2^-$ molecules when $^{\bullet}O_2^-$ is produced at the titania surface from adsorbed O_2.

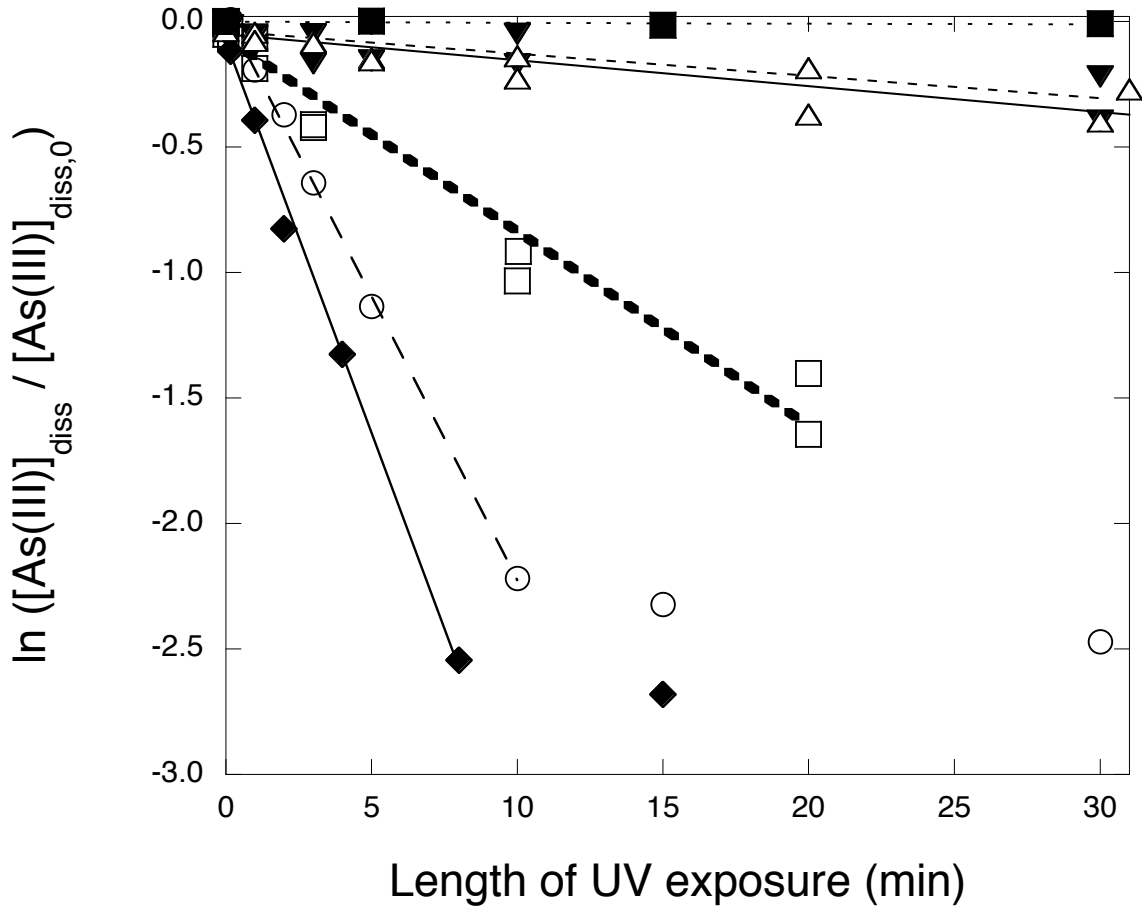

Figure 3.4. Comparison of As(III) oxidation under two experimental conditions designed to eliminate superoxide: N_2-saturated suspensions with 1.0 mM CCl_4 (△) and air-saturated suspensions with 100,000 units L^{-1} superoxide dismutase (□). Air-saturated experiments with 0 M phosphate (◆) and 10 μM phosphate (○), N_2-saturated experiments (▼), and dark control (■) are shown for comparison. Conditions: 0.83 μM As_T, pH 6.3, 0.05 g L^{-1} TiO_2, 0.005 M $NaNO_3$.

3.4.4 Implications for water treatment

The need to supply drinking water with As concentrations below 10 μg L^{-1} will require many water treatment facilities to implement additional As removal methods, most of which involve oxidation of As(III) to As(V) before further treatment. It is anticipated that small water supply systems will be disproportionately burdened by the

new drinking water standard for As (US EPA 2002d). Although TiO_2 photocatalysis is a novel technology for water treatment, UV disinfection is recommended by the U.S. Environmental Protection Agency for use in small water supply systems based on its relatively low cost, minimal chemical requirements, simple operation and maintenance, and small footprint (US EPA 2003b). These advantages would also be realized by small systems implementing TiO_2 photocatalysis for As(III) oxidation.

Understanding the implications of our study, as well as previous studies of TiO_2-photocatalyzed As(III) oxidation, for applications in water treatment requires consideration of the effects of source water composition and reactor design on process efficiency. Source water composition (including pH) can affect the extent of As(III) sorption onto TiO_2. The pH condition selected for our study, pH 6.3, is low compared to the pH range typical of sourcewaters, pH 6.5–8.5, but is more representative of average sourcewater conditions than the pH values of 3 or 9 used in the detailed mechanistic studies of this process (Lee and Choi 2002; Ryu and Choi 2004). Lee and Choi (2002) observed comparable adsorption of As(III) and As(V) on TiO_2 at pH 3; the extent of As(III) adsorption at pH 9 was comparable to that at pH 3 while As(V) adsorption was negligible at pH 9. Thus, the photooxidation rate should also remain relatively constant. Previous studies, despite the poor constraint on pH, support this hypothesis (Bissen et al. 2001; Lee and Choi 2002; Jayaweera et al. 2003; Ryu and Choi 2004).

A drinking water standard for As of 50 $\mu g\ L^{-1}$ (0.67 μM) has been in force in the U.S. since 1942. Thus, water supply systems whose source waters met the former standard but require treatment to meet the new standard will generally be treating water with As concentrations at or below this level. In our study, the TiO_2 photocatalyzed

oxidation of As(III) was driven to completion in less than 10 min with an initial As(III) concentration of 0.83 μM. However, our study also illustrates that the effects of initial As(III) concentration and the TiO_2 loading on the timescale of the photooxidation reaction reflects the nonlinear relationship of adsorbed and dissolved As(III) concentrations. Thus, the extent of As(III) adsorption and TiO_2 saturation must be evaluated for potential water treatment systems.

Batch reactor systems may provide insight into factors influencing the rates of TiO_2 photocatalyzed oxidation of As(III) but they rarely correspond to practical reactor designs for water treatment. For a continuous-flow system, with TiO_2 immobilized on a fixed bed, mass transport considerations must also be taken into account. However, our batch studies do indicate that the reversible adsorption of As(III), As(V), and phosphate should preclude irreversible poisoning of the catalyst even though As(III) photooxidation rates may be slowed by competitive effects.

3.5 Acknowledgements

We thank Dr. A. J. Colussi for helpful discussions and suggestions concerning this work. Financial support from the U.S. Environmental Protection Agency's Science to Achieve Results program (91596201-0) is gratefully acknowledged.

3.6 Addendum

Since the work detailed above was completed, three papers that also consider the mechanism of TiO_2-photocatalyzed As(III) oxidation have been published. These papers argue that oxidation by $^{\bullet}OH$ (Dutta et al. 2005; Xu et al. 2005) or h^+_{VB} (Yoon and Lee 2005) is dominant. These conclusions contrast with results from this study and other work (Lee and Choi 2002; Ryu and Choi 2004), so further discussion on the As(III) photooxidation reaction mechanism is warranted.

All three recent papers focused on adding reagents that scavenged $^{\bullet}OH$, h^+_{VB}, or e^-_{CB} from P25 TiO_2 slurries irradiated with UV light. Dutta et al. (2005) and Yoon and Lee (2005) both conducted experiments under sorption saturation conditions over a pH range of 3–9 or 3–11, whereas the experiments of Xu et al. (2005) were performed in the linear portion of the sorption isotherm at unstated pH. Benzoic acid, a $^{\bullet}OH$ quencher, slowed As(III) photooxidation by about 33%, and experiments measuring benzoic acid degradation exhibited a delay when As(III) was present (Dutta et al. 2005). In contrast, methanol, another $^{\bullet}OH$ scavenger, had no effect on As(III) photooxidation, but addition of hole scavengers oxalate, formate, and iodide significantly inhibited the reaction. As(III) inhibited the degradation of benzoate, terephthalate, and formate more strongly than methanol (Yoon and Lee 2005).

Systems using alternate electron acceptors, conducted in the nominal absence of O_2 (sparged with N_2 or Ar), were designed to eliminate formation of superoxide ($O_2^{\bullet-}$). As(III) photooxidation slowed but was still significant when Cu(I) or $SiW_{12}O_{40}^{4-}$ (polyoxometalate, POM) was added (Xu et al. 2005), whereas Cu(II) and BrO_3^- increased the As(III) reaction rate (Yoon and Lee 2005).

Pulse radiolysis was used to generate $^{\bullet}OH$, which subsequently adsorbed onto colloidal TiO_2 and was detected spectrophotometrically. This signal was muted when As(III) was added to the suspension (Xu et al. 2005).

Finally, all three recent studies incorporated a study of As(III) oxidation by $^{\bullet}OH$ and $O_2^{\bullet-}$ in homogeneous solution. Generation of these 2 reactive species using nitrate photolysis (Dutta et al. 2005), pulse radiolysis (Xu et al. 2005), and photooxidation of H_2O_2 (Yoon and Lee 2005) have reconfirmed previously reported data; that is, the rate of As(III) reaction with $^{\bullet}OH$ is 3 orders of magnitude higher than that with $O_2^{\bullet-}$ in homogeneous solution (Buxton et al. 1988a; Klaning et al. 1989). The microenvironment at the solid-liquid interface can have different pH and redox potential compared to values calculated in bulk solution, but it is still unknown whether the surface environment could cause the reactions of As(III) with $^{\bullet}OH_{ads}$ or $O_2^{\bullet-}{}_{ads}$ to be kinetically competitive with each other.

Table 3.3 summarizes the reaction conditions and effects of reagents added to UV-irradiated As(III)/TiO_2 systems to target the $^{\bullet}OH$, h^+_{VB}, or $O_2^{\bullet-}$-mediated reaction pathways in each of the six studies dedicated to determining the reaction mechanism. Lines C1–C5 correspond to addition of $^{\bullet}OH$ scavengers, which, after sorption effects were accounted for, either had no effect or caused the reaction to slow by about 33%. Based on the rate constants for homogeneous solutions reported in Table 3.4 (R1–R5) and the excess of $^{\bullet}OH$ quenchers used in C1–C5, *tert*-butanol (*t*-BuOH), 2-propanol, methanol, and benzoic acid should all participate in significant competition with As(III) if As(III) reacts via a $^{\bullet}OH$-induced mechanism. However, the homogeneous rate constants in Table 3.4 may not necessarily correspond to reactions with $^{\bullet}OH_{ads}$.

Table 3.3. Reagents added to elucidate the As(III) photooxidation reaction mechanism and their effects compared to the As(III)/TiO_2/Air/UV system. All solutions are bubbled with air and exposed to UV light unless stated otherwise.

		Initial [As(III)]	TiO_2 Loading	pH	Additional Reagent	Effect of Reagent
$^{\bullet}OH$ Quenchers	C1[a]	500 μM	1.5 g L^{-1}	3, 9	530 mM *t*-BuOH	No significant effect
	C2[c]	2.5 μM	0.05 g L^{-1}	6.4	100 mM *t*-BuOH 10 mM *t*-BuOH 1 mM *t*-BuOH	Decreased by 56%[g] Decreased by 42%[g] No significant effect
	C3[c]	2.5 μM	0.05 g L^{-1}	6.4	100 mM 2-propanol 1 mM 2-propanol	Decreased by 48%[g] Decreased by 33%
	C4[f]	100 μM	0.1 g L^{-1}	3, 7, 11	10 mM methanol	No significant effect
	C5[d]	200 μM	0.1 g L^{-1}	4	0.25 mM or 1.5 mM benzoic acid	Decreased by ~33%[h]
h^{+}_{VB} Quenchers	C6[f]	100 μM	0.01 g L^{-1}	3	0.3 mM oxalate / sparged with O_2	Decreased by ~87%
	C7[f]	100 μM	0.01 g L^{-1}	3	0.3 mM formate / sparged with O_2	Decreased by ~56%
	C8[f]	100 μM	0.1 g L^{-1}	3 7 11	2 mM KI / air-equilibrated	Decreased by ~88% Decreased by ~70% No significant effect
Alternate Electron Acceptors	C9[b]	500 μM	0.5 g L^{-1}	9	5 mM CCl_4 / sparged with N_2	Greatly decreased; same as N_2 control
	C10[c]	2.5 μM	0.05 g L^{-1}	6.4	1.0 mM CCl_4 / sparged with N_2	Decreased by 96%; almost the same as N_2 control
	C11[e]	13.4 μM	0.1 g L^{-1}	Not given	1.34 mM Cu^{+} / Ar-saturated	Slightly decreased
	C12[f]	100 μM	0.01 g L^{-1}	3	0.2 mM $Cu(NO_3)_2$ / air-equilibrated 0.2 mM $Cu(NO_3)_2$ / N_2-purged	Increased 5.9-fold Increased by ~55%
	C13[e]	13.4 μM	0.1 g L^{-1}	Not given	134 mM $SiW_{12}O_{40}^{4-}$ / Ar-saturated	Decreased by ~50%
	C14[f]	100 μM	0.1 g L^{-1}	3 7 11	0.3 mM $KBrO_3$ / sparged with N_2	Increased 5.3-fold Decreased by ~20% Decreased by ~60%

a: Lee and Choi, 2002
b: Ryu and Choi, 2004
c: This chapter
d: Dutta et al., 2005
e: Xu et al., 2005
f: Yoon and Lee, 2005
g: Decreased sorption of As(III) to TiO_2 accounted for all or part of this decrease in the reaction.
h: This reaction took 15 min to complete rather than 10 min for air/TiO_2/UV. However, the N_2/TiO_2/UV control only required 20 min for reaction completion.

Table 3.4. Reaction rate constants with $^{\bullet}OH$ radicals in homogeneous solution.

	Reaction	Rate Constant
R1	$As(OH)_3 + {}^{\bullet}OH \rightarrow As^{IV}(OH)_4$	$1.8–8.5 \times 10^9$ M^{-1} s^{-1} (a, b)
R2	t-BuOH + $^{\bullet}OH \rightarrow$ products	6.0×10^8 M^{-1} s^{-1} (b)
R3	2-propanol + $^{\bullet}OH \rightarrow$ products	1.9×10^9 M^{-1} s^{-1} (b)
R4	Methanol + $^{\bullet}OH \rightarrow H_2O + {}^{\bullet}CH_2OH$	9.7×10^8 M^{-1} s^{-1} (b)
R5	Benzoic acid + $^{\bullet}OH \rightarrow$ salicylic acid	5.9×10^9 M^{-1} s^{-1} (b)

(a) (Klaning et al. 1989)
(b) (Buxton et al. 1988a)

Alternatively, As(III) could be oxidized by direct electron transfer to valence band holes. Conditions C6–C8 in Table 3.3 document addition of hole scavengers, all of which substantially decreased As(III) oxidation.

Systems using alternate electron acceptors are detailed in lines C9–C14. Effects of these alternate electron acceptors ranged from nearly complete inhibition of the reaction in the case of CCl_4 to an increase in reaction rate by a factor of 5.3 when BrO_3^- was used. Both studies employing CCl_4 as an alternate electron acceptor found that the rate of As(III) reaction slowed to that of the N_2 control and cited this lack of reaction as indication that the superoxide pathway is dominant. Furthermore, Ryu and Choi (2004) measured 80 μM of Cl^- in solution at the end of their experiment and cited this as proof that CCl_4 was indeed acting as an electron acceptor. However, despite the much slower As(III) oxidation, about 65 μM of As(V) *is* generated in this system (As_T = 500 μM). Therefore, it appears that electron scavenging by CCl_4 may not be fast enough in this system to compare to the air-saturated system. In contrast, electron transfer to Cu(I), Cu(II), BrO_3-, and POM appears to be rapid enough to promote significant As(III) oxidation even in the nominal absence of O_2. The increased reaction rates observed for

Cu(II) and BrO_3^- support the hypothesis that electron transfer to O_2 is rate limiting (Gerischer and Heller 1991).

The above data imply that reaction with valence band holes can completely account for As(III) photooxidation on TiO_2. However, this work and other studies have also provided compelling evidence for As(III) reaction with $O_2^{\bullet-}$. Superoxide dismutase, which has been previously discussed, slowed As(III) oxidation by 55–73%. Choi and co-workers (2004) present several lines of evidence supporting a superoxide-based mechanism; the two strongest arguments are summarized below.

When added at 10 mg L^{-1}, humic acid increased the rate of As(III) photooxidation (Fig. 3.5) without affecting the sorption isotherms for As(III) or As(V). This effect was attributed to facilitation of electron transfer to O_2 by humic acid. Much higher dissolved concentrations of H_2O_2 were observed in the presence of humic acid (>150 μM) than in the absence of humic acid (< 10 μM). The authors argue that this supports additional superoxide formation, leading to enhanced H_2O_2 production according to the following reaction:

$$As(OH)_3 + O_2^{\bullet-} + 2H^+ \rightarrow As^{IV}(OH)_3 + H_2O_2 \qquad (3.1)$$

In contrast to the authors' interpretation, one could suggest that humic acid causes formation of H_2O_2 via an As-independent mechanism (e.g., from humic acid radicals), but very little H_2O_2 was detected in the UV-irradiated TiO_2 system when As(III) was not present (Fig. 3.6). Alternatively, since H_2O_2 is produced independently on semiconductor surfaces (Kormann et al. 1988; Hoffman et al. 1994), the presence of humic acid could slow H_2O_2 degradation by competing for valence band holes or inhibiting the sorption of H_2O_2 to TiO_2. However, the pattern of H_2O_2 detected over time shows an increase in

H_2O_2 for the first hour of illumination, after which the H_2O_2 concentration steadily drops to <20 μM (Fig. 3.7). As(III) oxidation was complete within the same time frame (Fig. 3.5), indicating that As(III) photooxidation is the dominant source of H_2O_2 and that after most As(III) has reacted, the rate of H_2O_2 degradation surpasses that of H_2O_2 generation. Moreover, the addition of *t*-BuOH prevents loss of H_2O_2, whereas it causes only a slight decrease in the As(III) oxidation rate. The lower As(III) reaction efficiency in the presence of *t*-BuOH may be due to scavenging of free $^{\bullet}OH$ generated by decomposition of H_2O_2, but As(III) oxidation in the presence of both humic acid and *t*-BuOH still proceeds more rapidly than in the system with only As(III) and TiO_2.

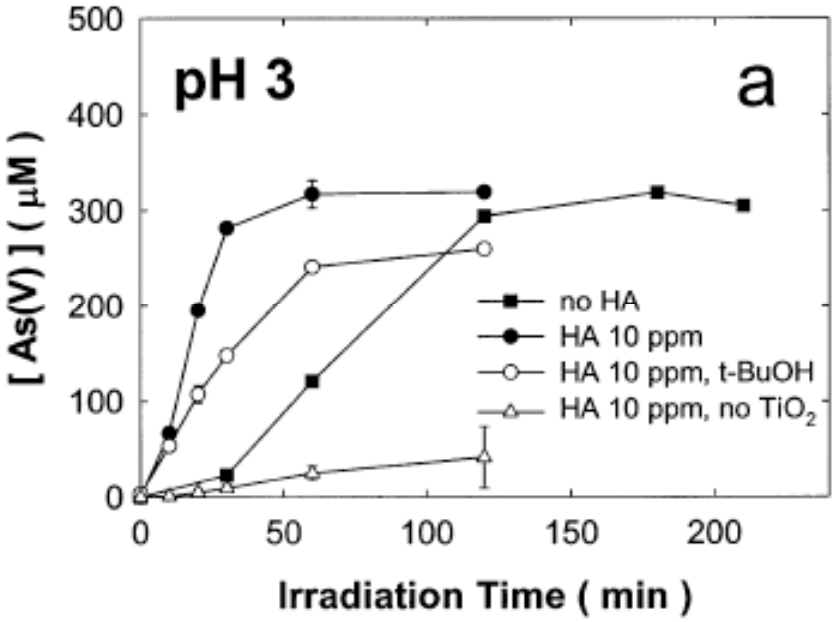

Figure 3.5. Photocatalytic oxidation of As(III) in the presence and absence of humic acid. Conditions: pH 3, 1.5 g L^{-1} P25 TiO_2, $[As(III)]_0$ = 500 μM, [humic acid] = 10 mg L^{-1}, [*t*-BuOH] = 0.53 M, air-equilibrated. Reprinted in part with permission from Lee and Choi (2002). Copyright (2002) American Chemical Society.

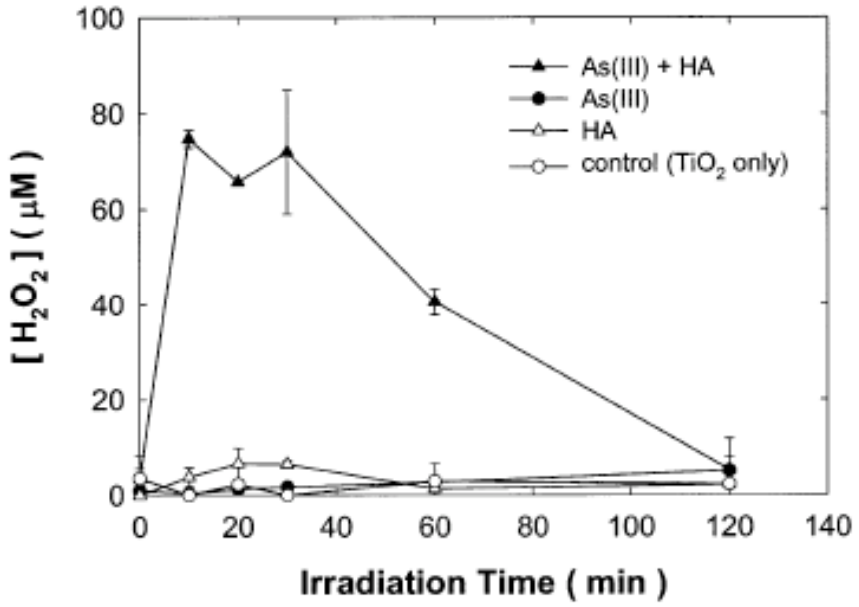

Figure 3.6. Time profiles of H_2O_2 production in UV-illuminated TiO_2 suspension compared in the presence of As(III), humic acid, or both. Conditions: pH 3, 1.5 g L^{-1} P25 TiO_2, $[As(III)]_0$ = 500 μM, [humic acid] = 10 mg L^{-1}, air-equilibrated. Reprinted in part with permission from Lee and Choi (2002). Copyright (2002) American Chemical Society.

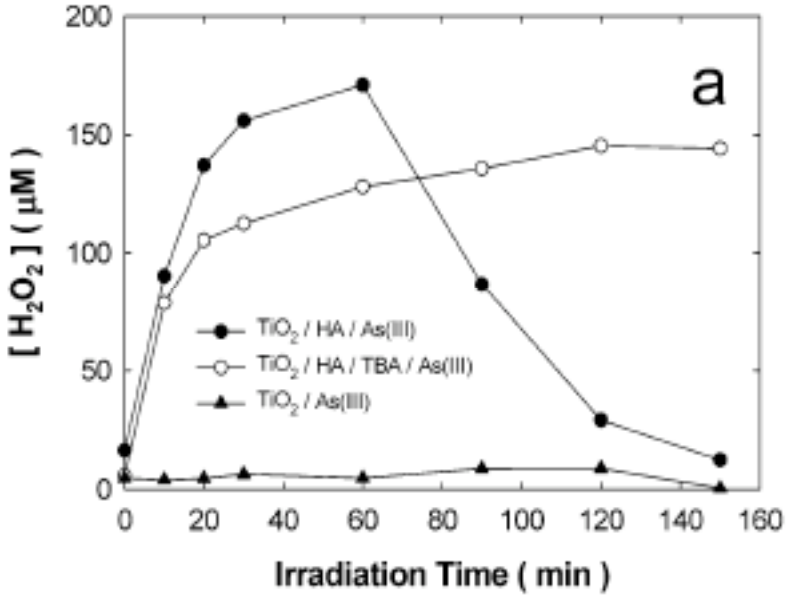

Figure 3.7. Time profiles of H_2O_2 production in the course of As(III) photooxidation in P25 TiO_2 suspensions. Conditions: pH 3, 0.5 g L^{-1} P25 TiO_2, $[As(III)]_0$ = 500 μM, [humic acid] = 10 mg L^{-1}, [*t*-BuOH] = 0.53 M, air-equilibrated. Reprinted in part with permission from Ryu and Choi (2004). Copyright (2004) American Chemical Society.

Experiments with the dye tris(4,4'-dicarboxy-2,2'-bipyridyl)ruthenium(II) ($Ru^{II}L_3$) on platinized TiO_2 (Pt-TiO_2) using visible light isolated reactions at the conduction band from those at the valence band. The Pt-TiO_2 system oxidizes As(III) only very slowly in visible light; this rate is equal to that of the same system in the dark. However, when $Ru^{II}L_3$ is included, As(V) generation under visible light nearly matches that of the As(III)/Pt-TiO_2 system under UV light. The authors suggest that the dye, which is adsorbed to the TiO_2, absorbs visible light and becomes excited, injecting an electron into the conduction band of TiO_2. This electron is then transferred efficiently to O_2 at the Pt-TiO_2 surface (Ryu and Choi 2004). Recent EPR studies (Yu et al. 2004) have confirmed superoxide generation on colloidal TiO_2 under visible irradiation in the presence of porphyin dyes. Since the valence band is not invoked in this system at all, these data present strong evidence in favor of the $O_2^{\bullet-}$-based mechanism, although this mechanism could be further substantiated if a control with only $Ru^{II}L_3$, As(III), visible light, and air were included.

Although the different studies considered here present conflicting hypotheses regarding which mechanism is dominant for As(III) photooxidation in the presence of TiO_2, no observation can unequivocally account for the entire As(III) oxidation reaction. The h^+_{VB}-dependent mechanism is strongly supported by substantial As(III) oxidation in N_2- or Ar-saturated solutions when Cu(I), Cu(II), POM, or BrO_3^- are present and by decreased As(III) photooxidation when the hole scavengers oxalate, formate, or iodide are present. The most powerful observations supporting the $O_2^{\bullet-}$-mediated mechanism are those experiments involving SOD, H_2O_2 generation when humic acid and As(III) are present, and dye exposed only to visible light. These data cumulatively suggest that

As(III) oxidation takes place by reactions with both h^{+}_{VB} and $O_2^{\bullet-}$, with each contributing significantly to the overall reaction. Since opposite charge carriers are involved in these two mechanisms, inhibiting one mechanism by scavenging holes or electrons is likely to favor the other due to decreased charge carrier recombination.